Submesoscale Frontogenesis, Arrest, and Decay: With and Without Surface Waves

J. McWilliams, UCLA

The oceanic submeoscale is a bunch of lines on the sea surface;
i.e., surfactants gathered into horizontal convergences above downwelling jets

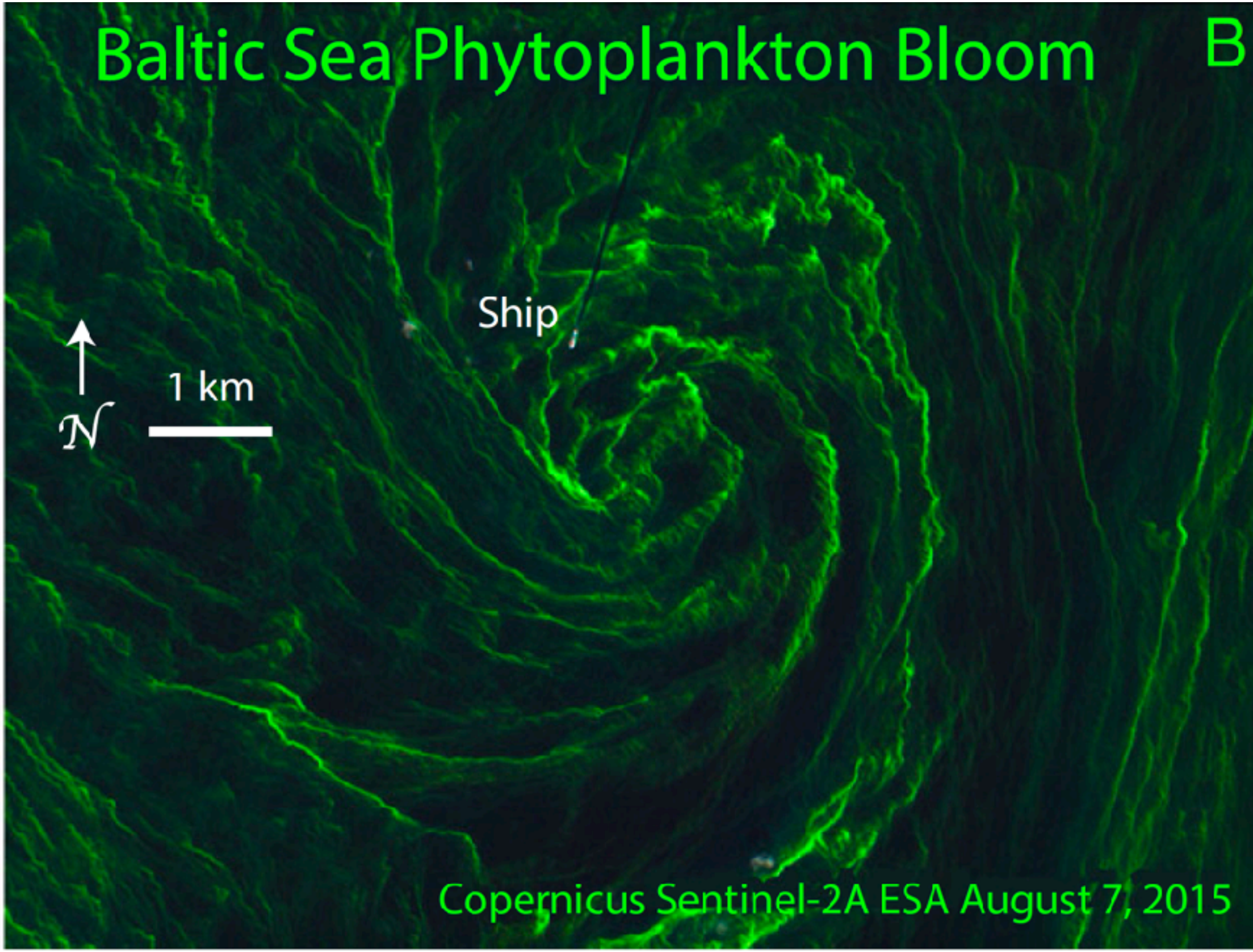

Spirals on the Sea

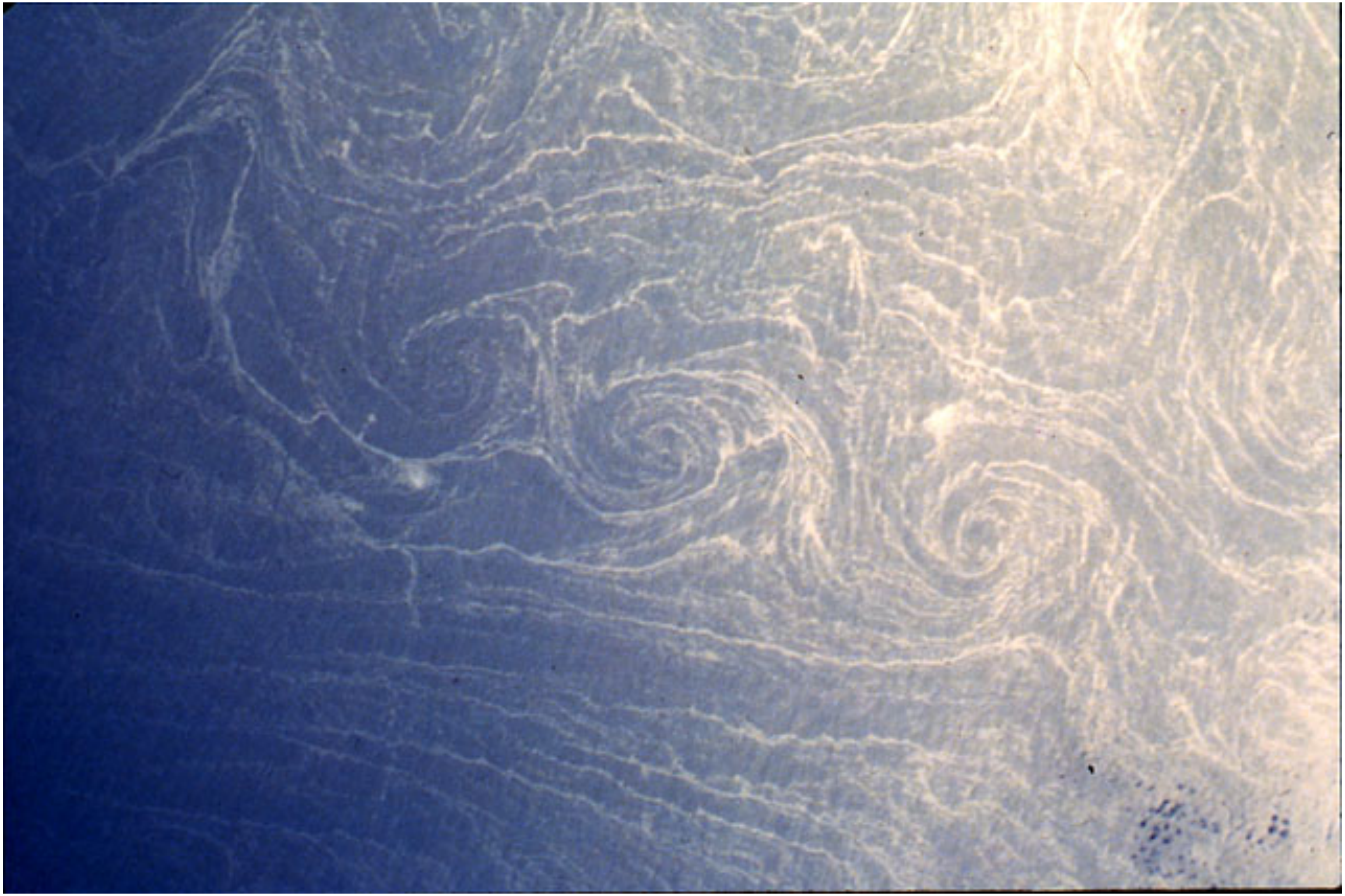

Sun-glint showing ~ 5 km ``spirals on the sea'' not far off the Mediterranean coast of Africa photographed from space (Scully-Power, 1986)

Lines are at density **filaments** (mimima) or density **fronts** (steps).

lines are horizontal density gradients, along-line jets,
and overturning secondary circulations

they arise from frontogenesis

the energy source is available potential energy, $wb > 0$,
while the processes of its release can be of several types

occasionally the lines roll up or tear apart into coherent vortices

$Ro, Fr, Ri \sim 1$

Frontogenesis induced by an ambient horizontal strain field
(a la Bergeron, Hoskins, …)

Density Front

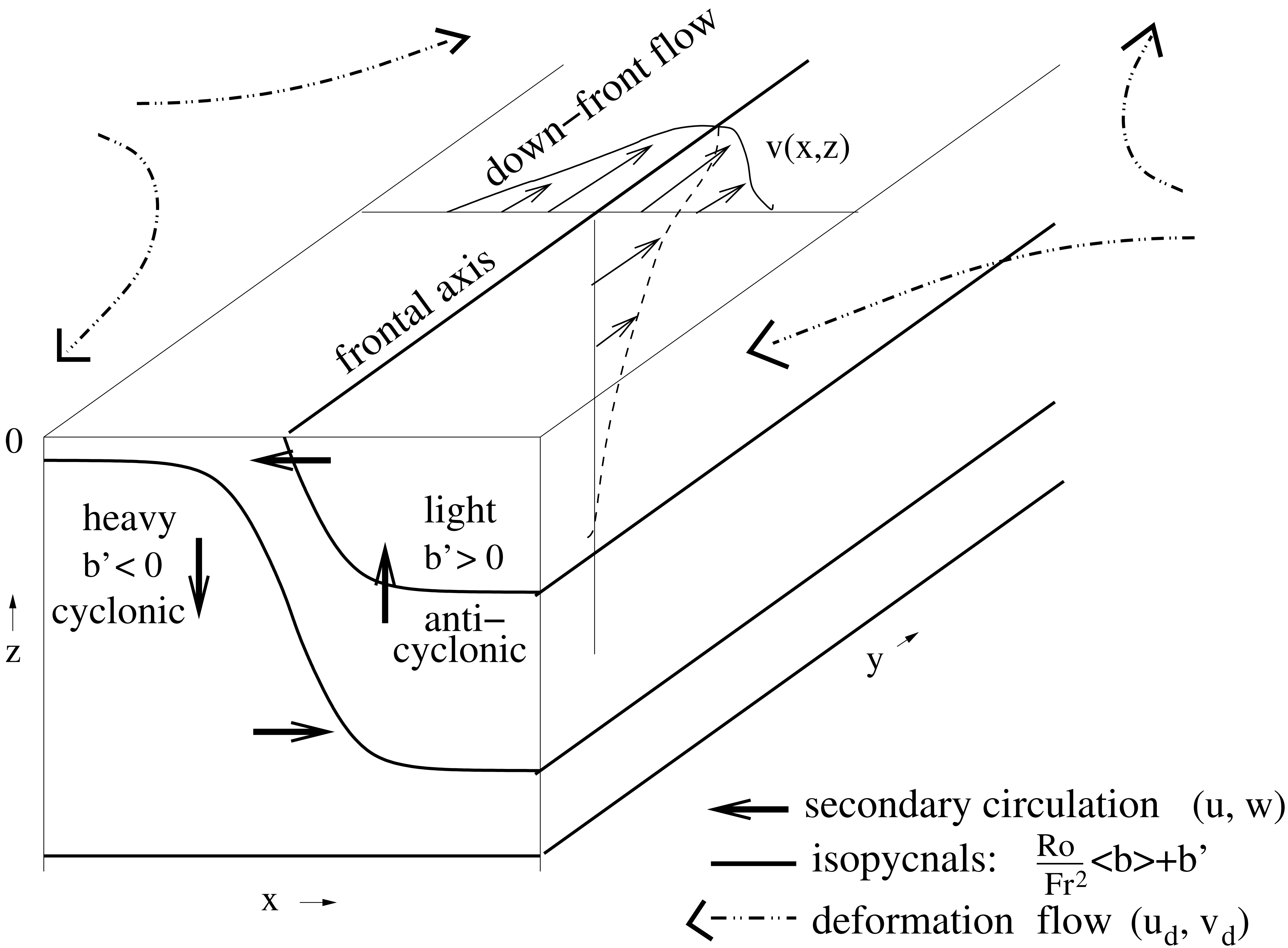

Density Filament

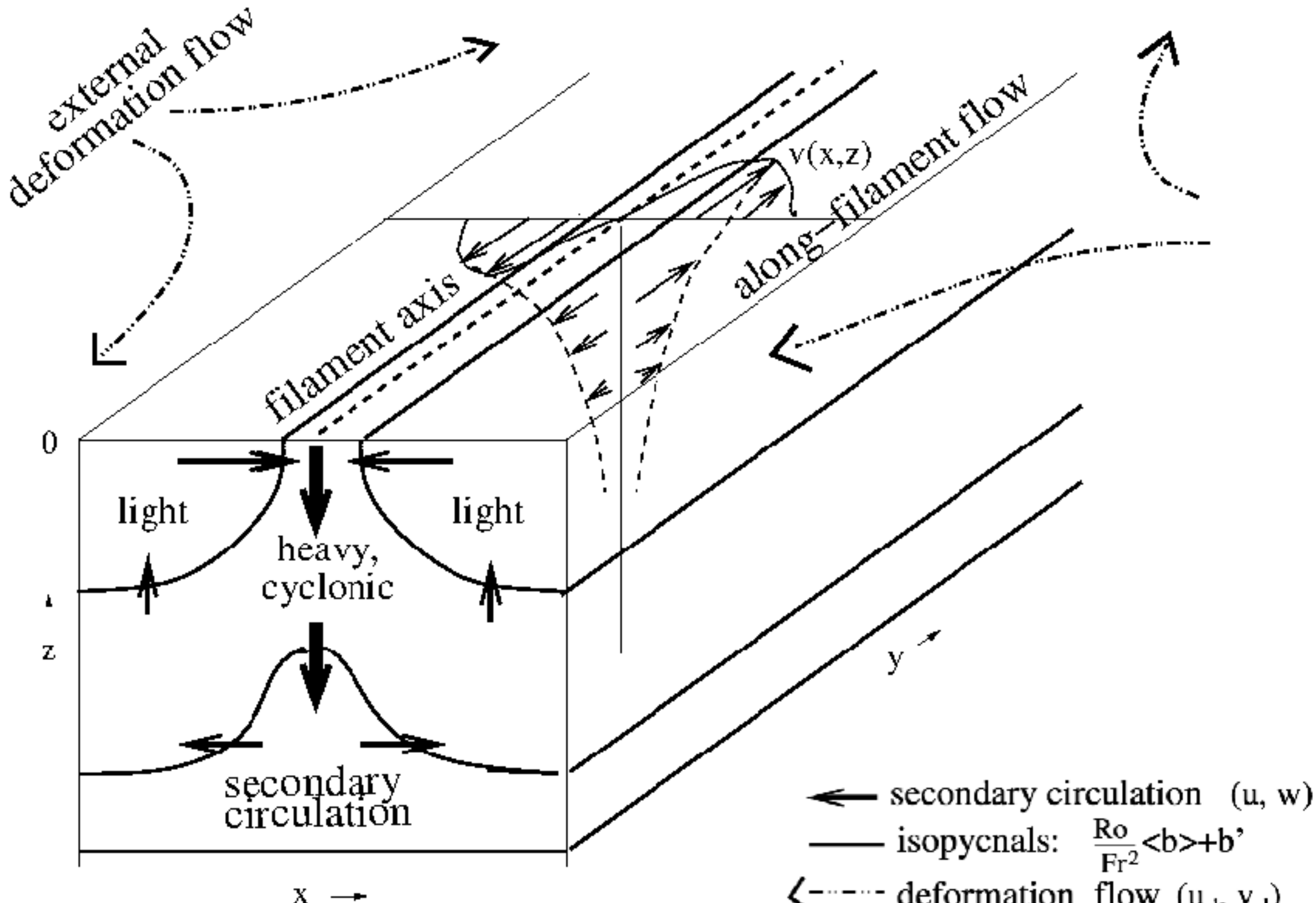

filaments have stronger convergence and frontogenesis per unit density gradient and strain

Convergence vs. Strain?

As an "external" velocity, both fields imply exponential growth for any passive $|\nabla c|$ ~ $|\nabla \rho|$.

As a local secondary circulation, convergence implies super-exponential growth for $|\nabla \rho|$.

Oceanic mesoscale and atmospheric synoptic-scale have stronger strain than convergence because $Ro \ll 1$.

Oceanic submesoscale fronts have both comparable strain and convergence because $Ro \gtrsim 1$.

Turbulent Thermal Wind Balance (TTW):

combined effects of a geostrophic shear and vertical momentum mixing

$$- \partial_z \left[\nu_v \partial_z u \right] - fv = - \partial_x \int^z b' \, dz$$

$$- \partial_z \left[\nu_v \partial_z v \right] + fu = - \partial_y \int^z b' \, dz$$

$$\partial_x u + \partial_y v + \partial_z w = 0$$

e.g., for $S = \partial_z v_g(z) > 0$ in the surface boundary layer ($z > -h$), TTW => the ageostrophic flow $\mathbf{u}_a(z)$ is left-rearward relative to $v_g(z)$.

=> in 2D $u_a(x,z)$ is a frontogenetic cross-frontal secondary circulation in the same sense as in strain-induced frontogenesis.

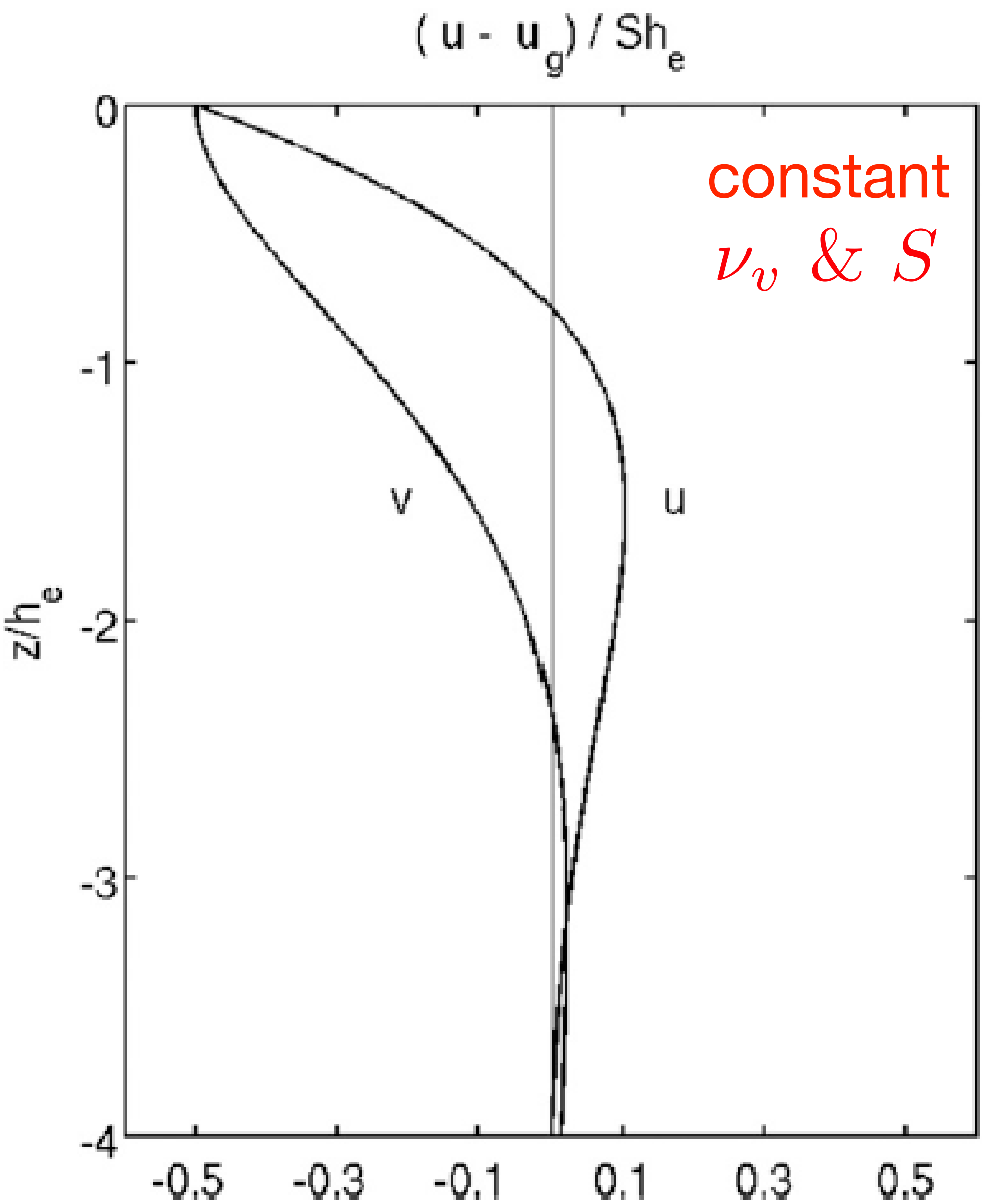

TTW is only an approximation to the balanced diagnostic model; e.g., it is not aware of stratification or ageostropihic advection.

Linear TTW without Wind or Waves

Front | Dense Filament

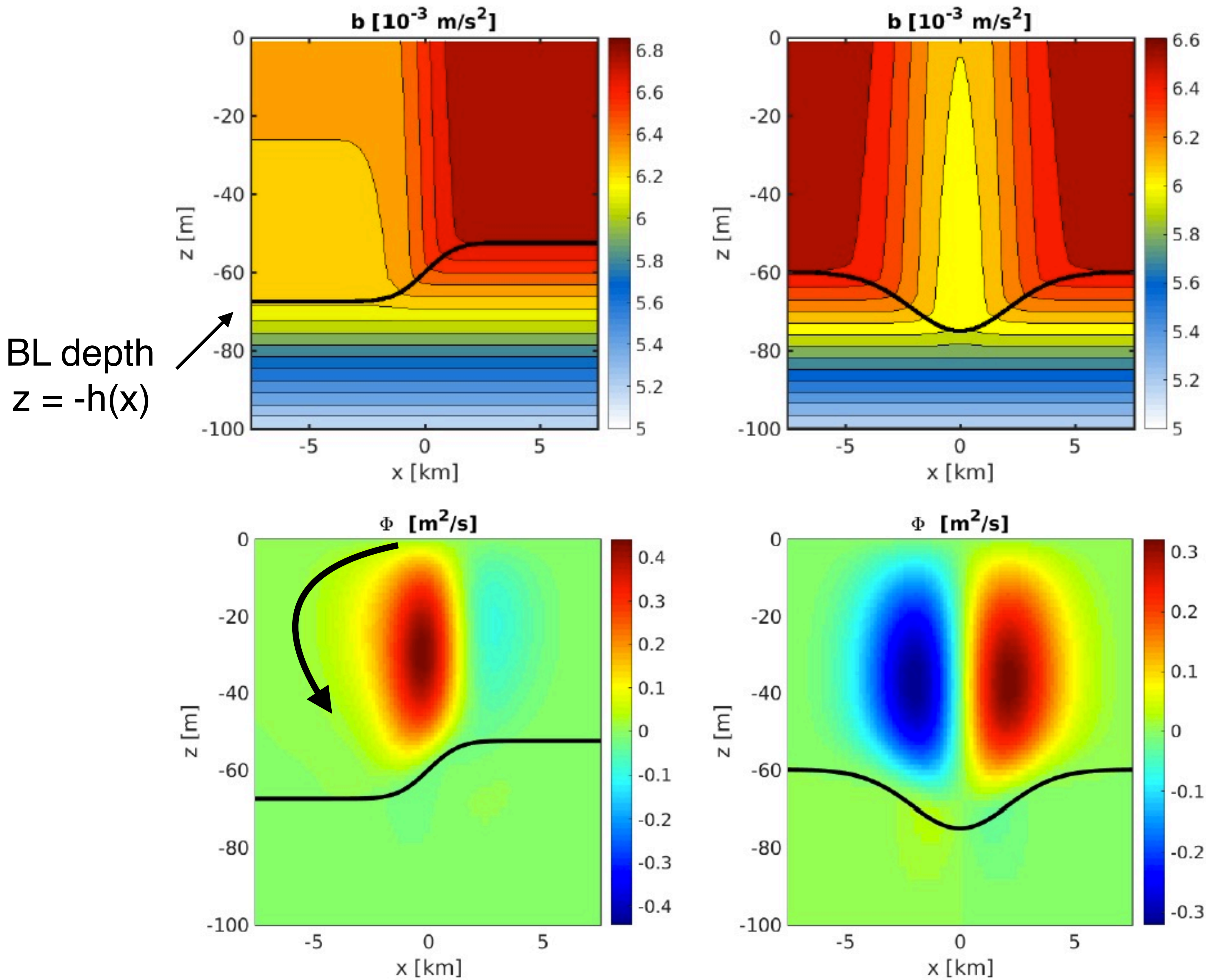

buoyancy field

"TTW" ageostrophic streamfunction for secondary circulation (u,w) (x,z)

convergence on dense side | convergence in center

Diagnosing Secondary Circulation and FrontogeneticTendency (SCFT)

After the circulation dynamics has created submesoscale coherent structures with only "slow" advective and boundary layer evolution rates, diagnose the instantaneous 3D

secondary circulation u_a
frontogenetic tendencies (T^b, T^u) $= \left(\frac{D|\nabla_h b|^2}{Dt}, \frac{D|\nabla_h \mathbf{u}_h|^2}{Dt} \right)$

from b(x,z) and the turbulent forcing and mixing ($\nu_v, \; \kappa_v(x,y), \; \boldsymbol{\tau}, \& \; Q$) by assuming, as the only dynamical approximation to the hydrostatic, incompressible Primitive Equations with vertical mixing and wave- averaged Stokes vortex forces, the **neglect of the ageostrophic time tendency** in the horizontal momentum equations.

This is a kind of maximally inclusive Balance Equations that excludes, e.g., inertia-gravity waves; i.e., a kind of generalized Sawyer-Eliassen model, but not based on the usual $\delta \ll \zeta = \partial_x v - \partial_y u$ approximation. Solved iteratively.

It does not preclude evolution in b and u_g, hence in u_a.

Its PDE solutions can be expected to fail to exist at some finite Ro > 1. The true evolution is presumed to stay close to this balanced state, as in realistic ROMS simulations.

Today SCFT is applied to 2D b(x,z) fronts and dense filaments.

(McWilliams, 2017)

SCFT Diagnostic Analysis:
Vertical Velocity in a Dense Filament

Linear TTW without wind

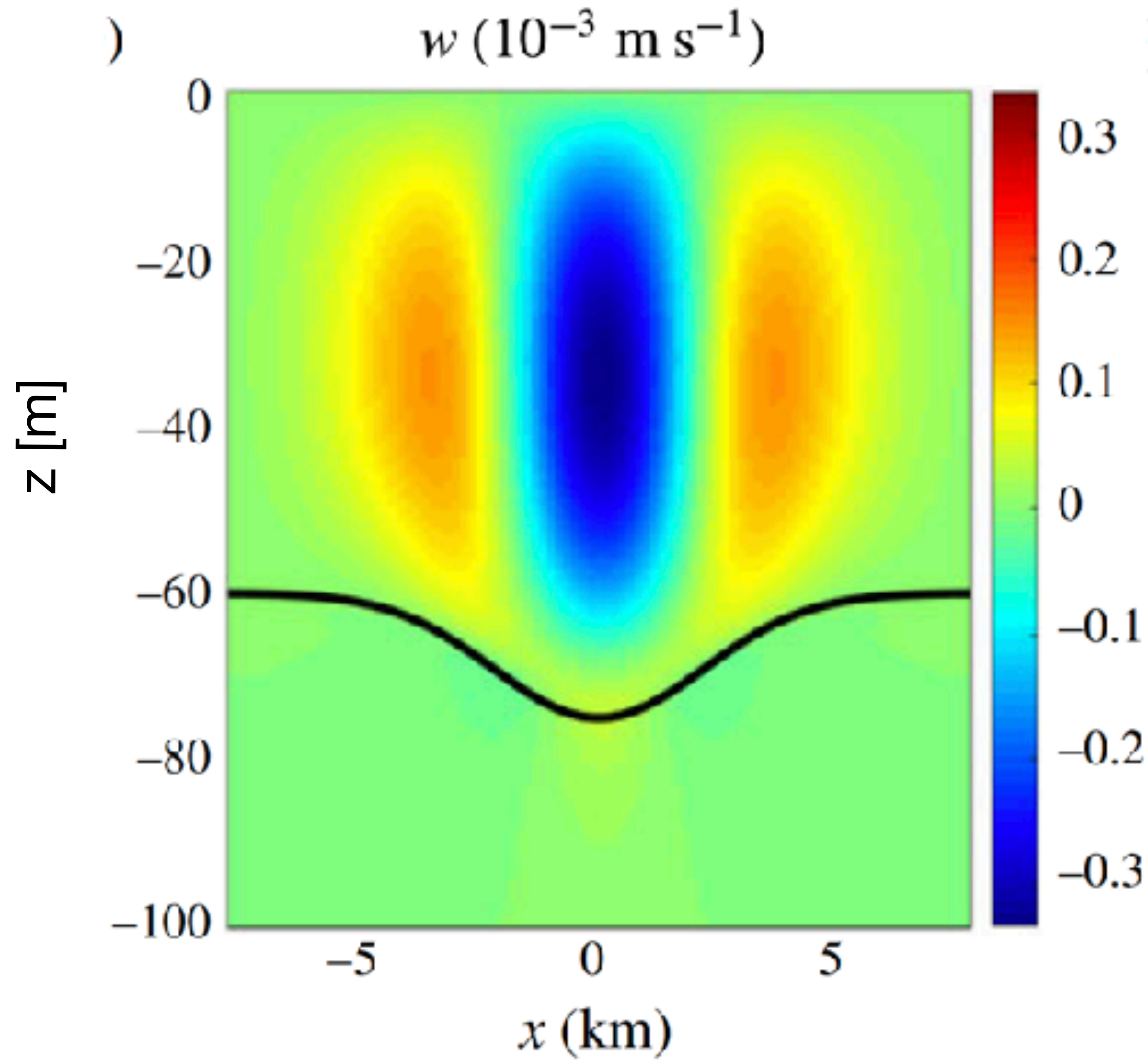

Nonlinear TTW with wind

$$\theta_w = \frac{\pi}{4} \quad (NE)$$

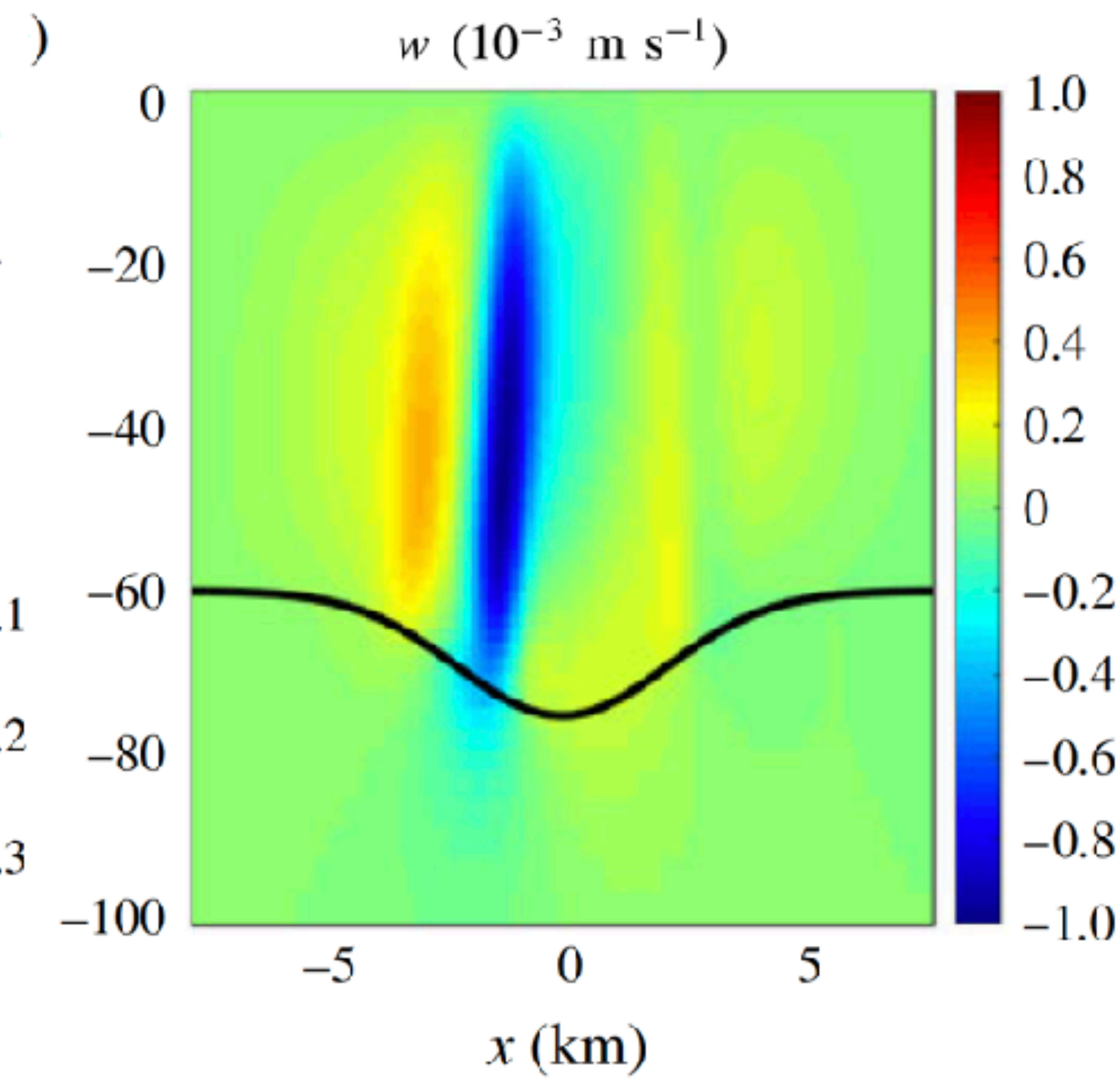

Simplified Theory of Strong Frontogenesis

Strain Induced Frontogenesis (Semigeostrophy) Scaling

Without loss of generality we assume the anisotropic submesoscale features are aligned in the y direction. Apply semigeostrophic scaling:

cross-front along-front mixed-layer depth

$$x \sim l, \qquad y \sim L, \qquad z \sim h_{\mathrm{ml}},$$

along-front cross-front

$$v \sim V, \qquad u \sim \epsilon V, \qquad w \sim u\frac{h_{\mathrm{ml}}}{l},$$

$$T \sim \frac{l}{\epsilon V}, \qquad \Phi \sim fVl, \qquad b \sim \frac{fVl}{h_{\mathrm{ml}}},$$

along-front geostrophic hydrostatic balance

$$\boxed{Ro = \frac{V}{fl} \sim O(1)} \qquad \boxed{\epsilon = \frac{l}{L} \ll 1}$$

(Hoskins and Bretherton, 1972)

Submesoscale Frontogenesis Scaling

motivated by the rapid frontogenetic time scales and comparable cross-front and along-front velocity magnitudes we use:

cross-front	along-front	mixed-layer depth
$x \sim l,$	$y \sim L,$	$z \sim h_{\mathrm{ml}},$

along-front

$$v \sim V,$$

cross-front

$$u \sim RoV,$$

$$w \sim u\frac{h_{\mathrm{ml}}}{l},$$

$$T \sim \frac{l}{RoV}, \qquad \Phi \sim fVl, \qquad b \sim \frac{fVl}{h_{\mathrm{ml}}},$$

along-front geostrophic hydrostatic balance

$$\boxed{Ro = \frac{V}{fl} \sim O(1)} \qquad \boxed{\epsilon = \frac{l}{L} \ll 1}$$

Frontogenetic Tendencies and Rates

buoyancy frontal tendency

$$\frac{D}{Dt}\frac{1}{2}|\nabla_h b|^2 = \underbrace{Q \cdot \nabla_h b}_{\mathcal{F}_b} \;\rightarrow\; \underbrace{-\delta|\nabla_h b|^2}_{\mathcal{F}_b}$$

new scaling

velocity frontal tendency

$$\frac{D}{Dt}\frac{1}{2}|\nabla_h \boldsymbol{u}_h|^2 = \mathcal{F}_{\boldsymbol{u}} \;\rightarrow\; \underbrace{-\delta|\nabla_h \boldsymbol{u}_h|^2}_{\mathcal{F}_{\boldsymbol{u}}}$$

frontogenetic tendency rates

$$\mathcal{T}_b = \frac{\mathcal{F}_b}{|\nabla_h b|^2}, \quad \mathcal{T}_{\boldsymbol{u}} = \frac{\mathcal{F}_{\boldsymbol{u}}}{|\nabla_h \boldsymbol{u}|^2}$$

$$\boxed{\mathcal{T}_b \approx \mathcal{T}_{\boldsymbol{u}} \approx -\delta}$$

$$\delta = u_x + v_y$$

What about the divergence evolution?

$$\frac{D}{Dt}\frac{1}{2}|\nabla_h b|^2 \approx \underbrace{-\delta|\nabla_h b|^2}_{\mathcal{F}_b} + \dots$$

frontogenetic rates

$$\frac{D}{Dt}\frac{1}{2}|\nabla_h \boldsymbol{u}_h|^2 \approx \underbrace{-\delta|\nabla_h \boldsymbol{u}_h|^2}_{\mathcal{F}_{\boldsymbol{u}}} + \dots$$

$$\frac{D}{Dt}\delta \approx -\delta^2 + f\zeta_{\mathrm{ag}} + V_{\mathrm{mix}} + V_{\mathrm{adv}} + H_{\mathrm{diff}}$$

after removing geostrophic balance

TTW balances

$$\frac{D}{Dt}\zeta = -\delta\zeta + f\delta + V_{\mathrm{mix}} + V_{\mathrm{adv}} + H_{\mathrm{diff}}$$

$\longrightarrow$ strong frontogenesis in a Lagrangian frame with $Ro \gg 1$:

$$\dot{\delta} = -\,\delta^2\ , \qquad \dot{\zeta} = -\,\delta\zeta\ .$$

with $\delta < 0\,,\ \zeta > 0$ at the center of the front (i.e., convergent and cyclonic).

$$\Rightarrow \quad \delta(t) \ \approx \ -\frac{1}{t_s - t}\ , \qquad \zeta(t) \ \propto \ +\frac{1}{t_s - t} \qquad \mathrm{as}\ t \to t_s^-\ .$$

a finite time singularity with -δ as its growth rate. Also,

$$\dot{|\nabla b|^2} = -\,\delta\,|\nabla b|^2 \quad \Rightarrow \quad |\nabla b|(t) \ \propto \ +\frac{1}{(t_s - t)^{1/2}}\ .$$

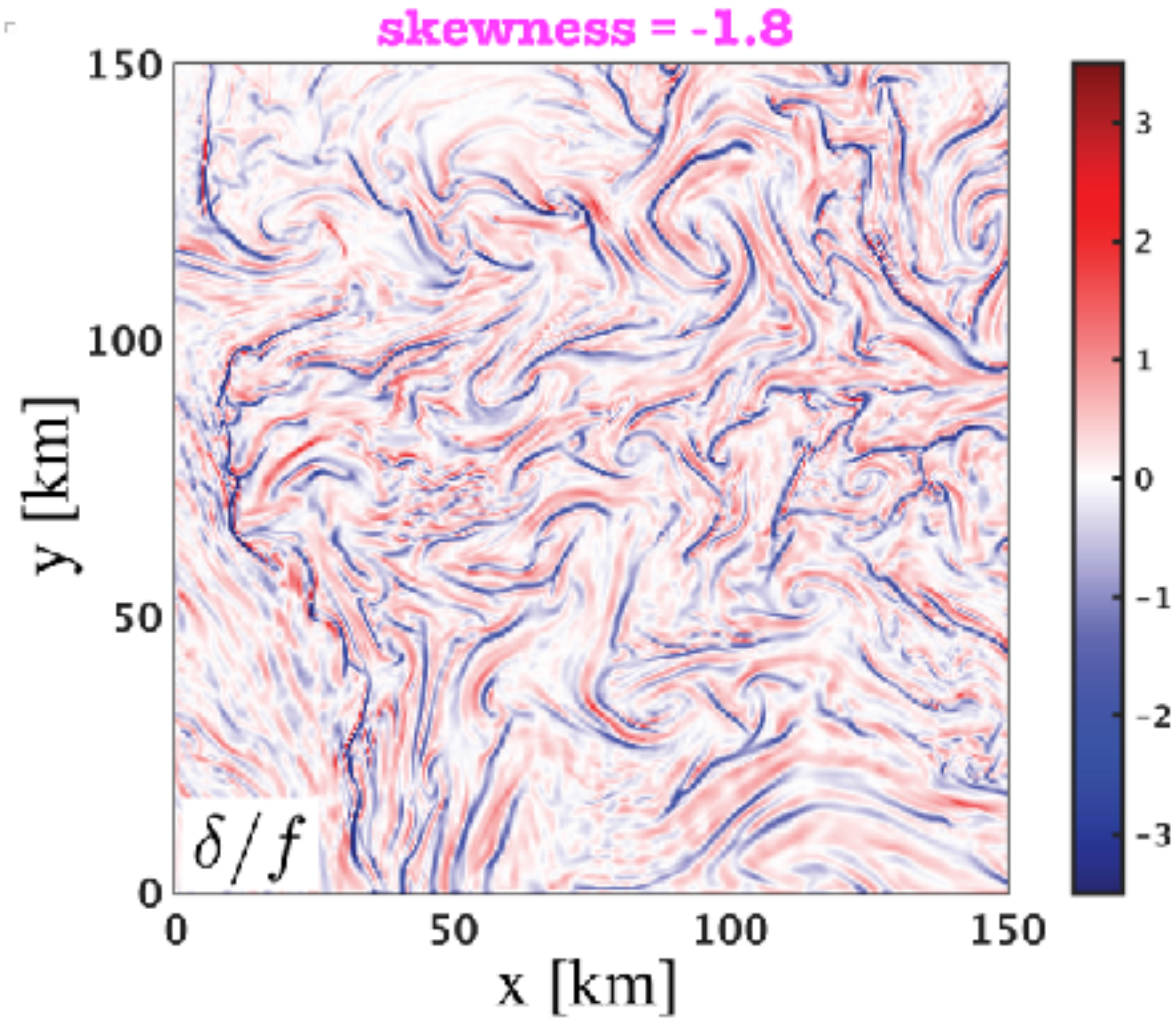

snapshot of surface divergence
in a realistic ROMS simulation
for the Gulf of Mexico

tests of asymptotic theory:
composite evolution over
656 detected frontogenesis
events in this simulation

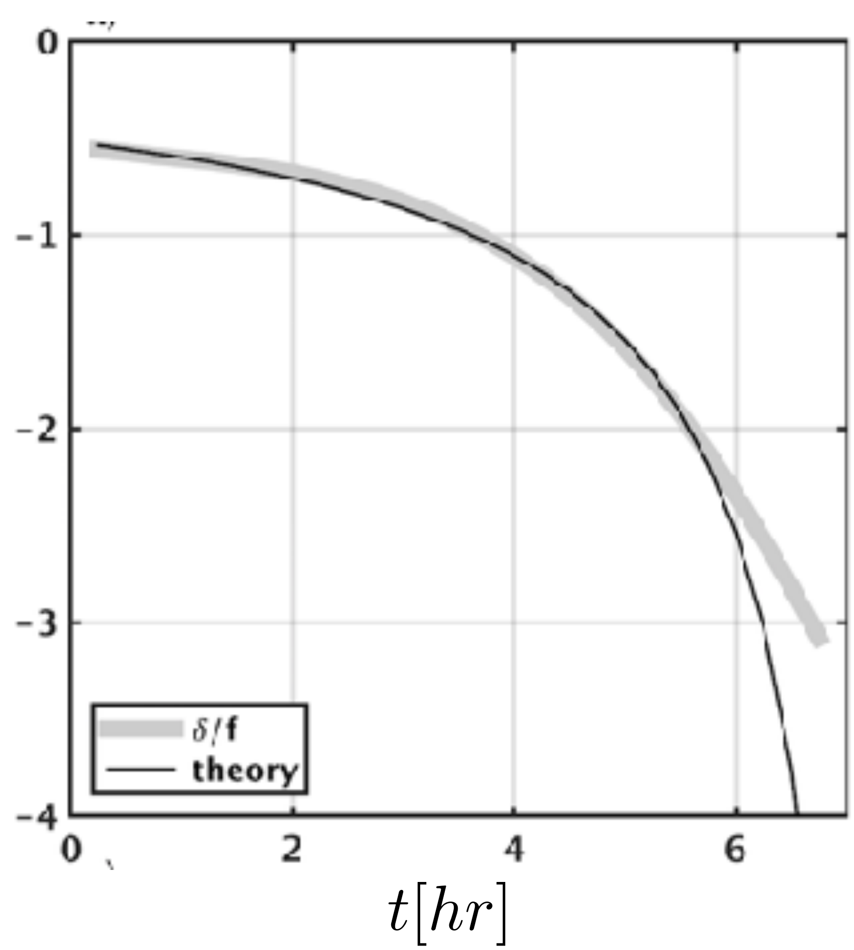

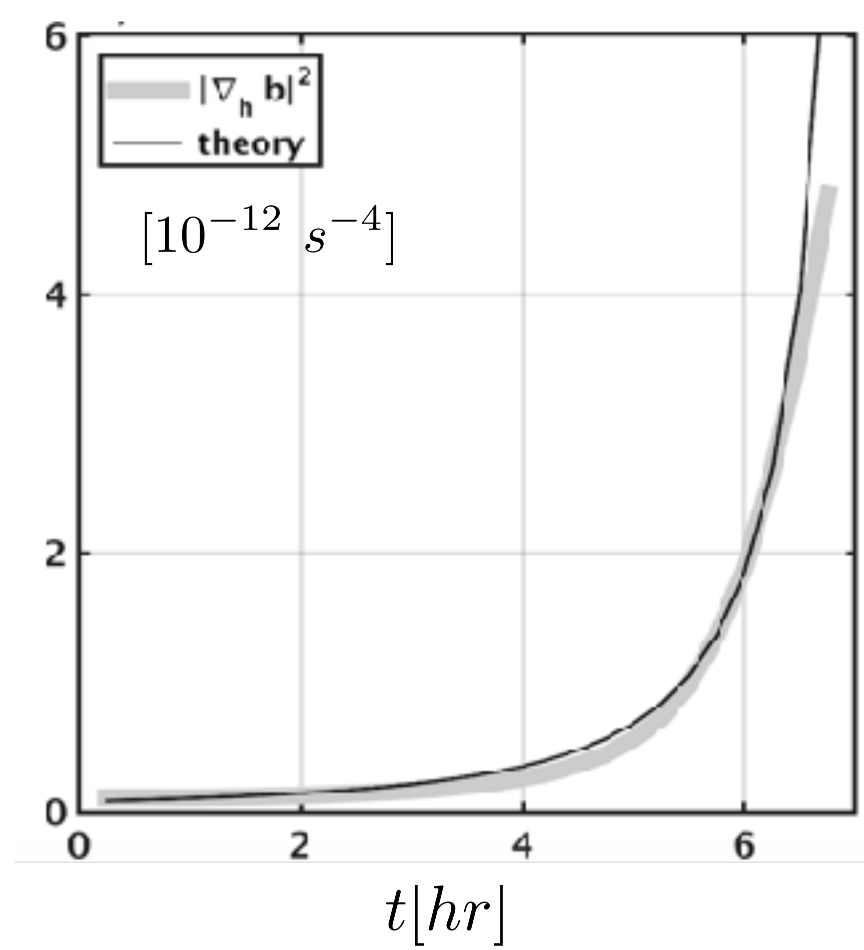

frontogenesis slows
at late time in model
due to instability
& diffusive arrest

(Barkan et al, 2018)

Large-Eddy Simulation: Filament Frontogenesis, Arrest, & Decay

boundary-layer turbulence generated by surface cooling

fully turbulent i.c.

at t= 6 hrs., peak frontal strength and arrest

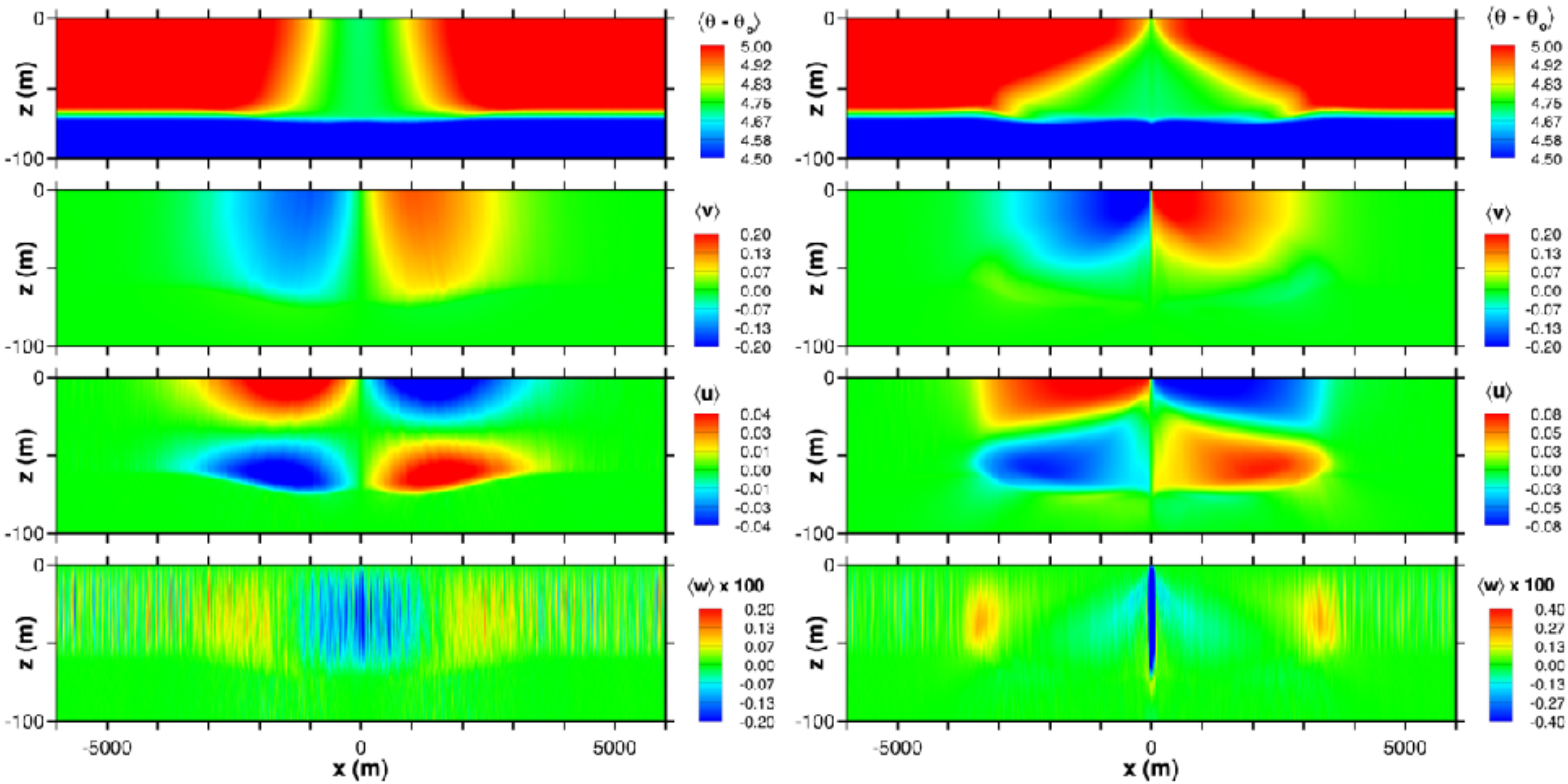

along-front averaged fields

(Sullivan & McWilliams, JFM, 2017)

Large-Eddy Simulation of Frontogenesis, Arrest, and Decay:

time series of y-averaged peak vorticity, w, and turbulent KE

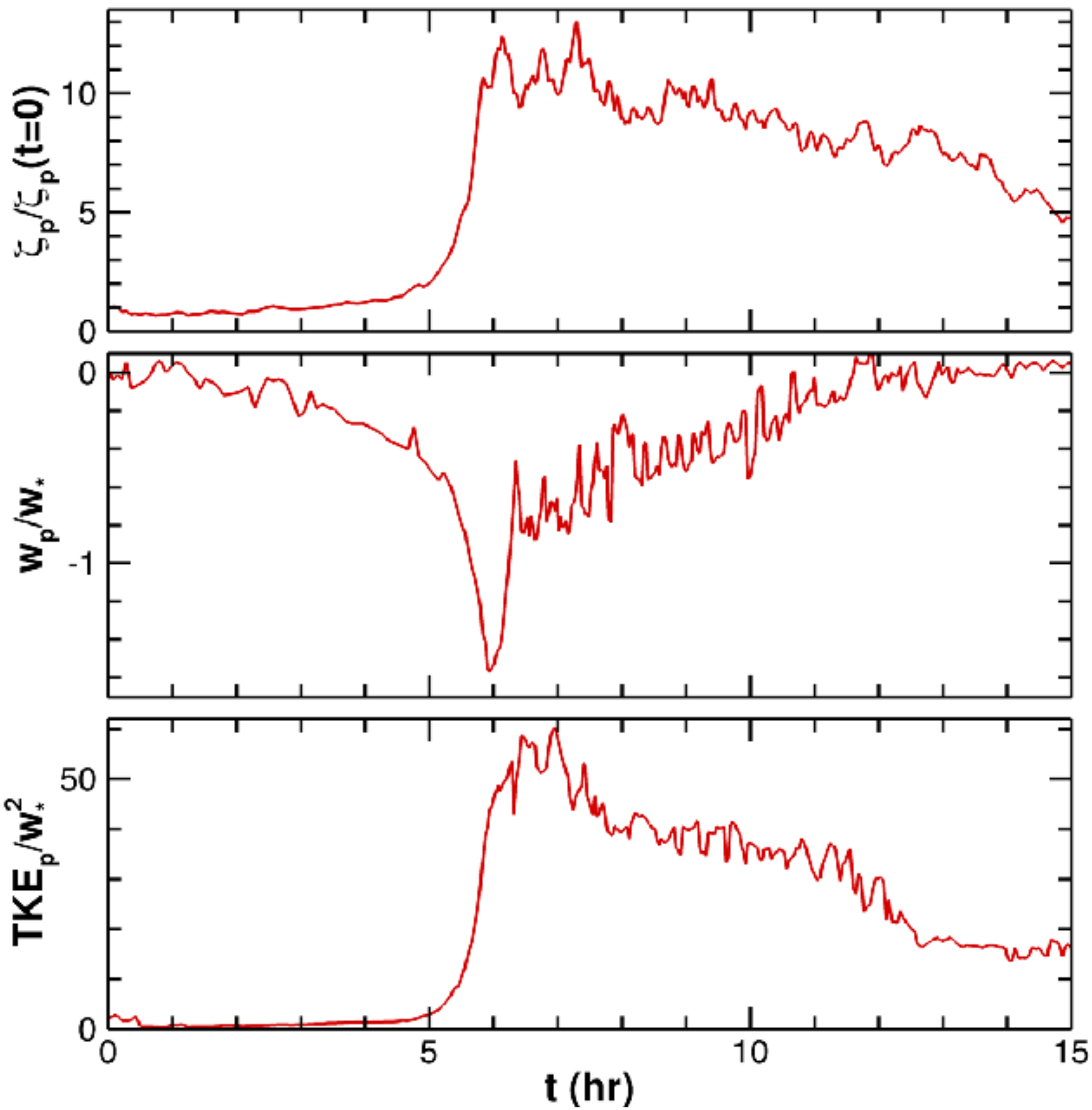

Large-Eddy Simulation of Frontogenesis, Arrest, & Decay:

near-surface $\mathbf{u}$ indicating arrest by horizontal shear instability of the sharp front

note the small arrest scale ~ 100 m ~ h_{bl}

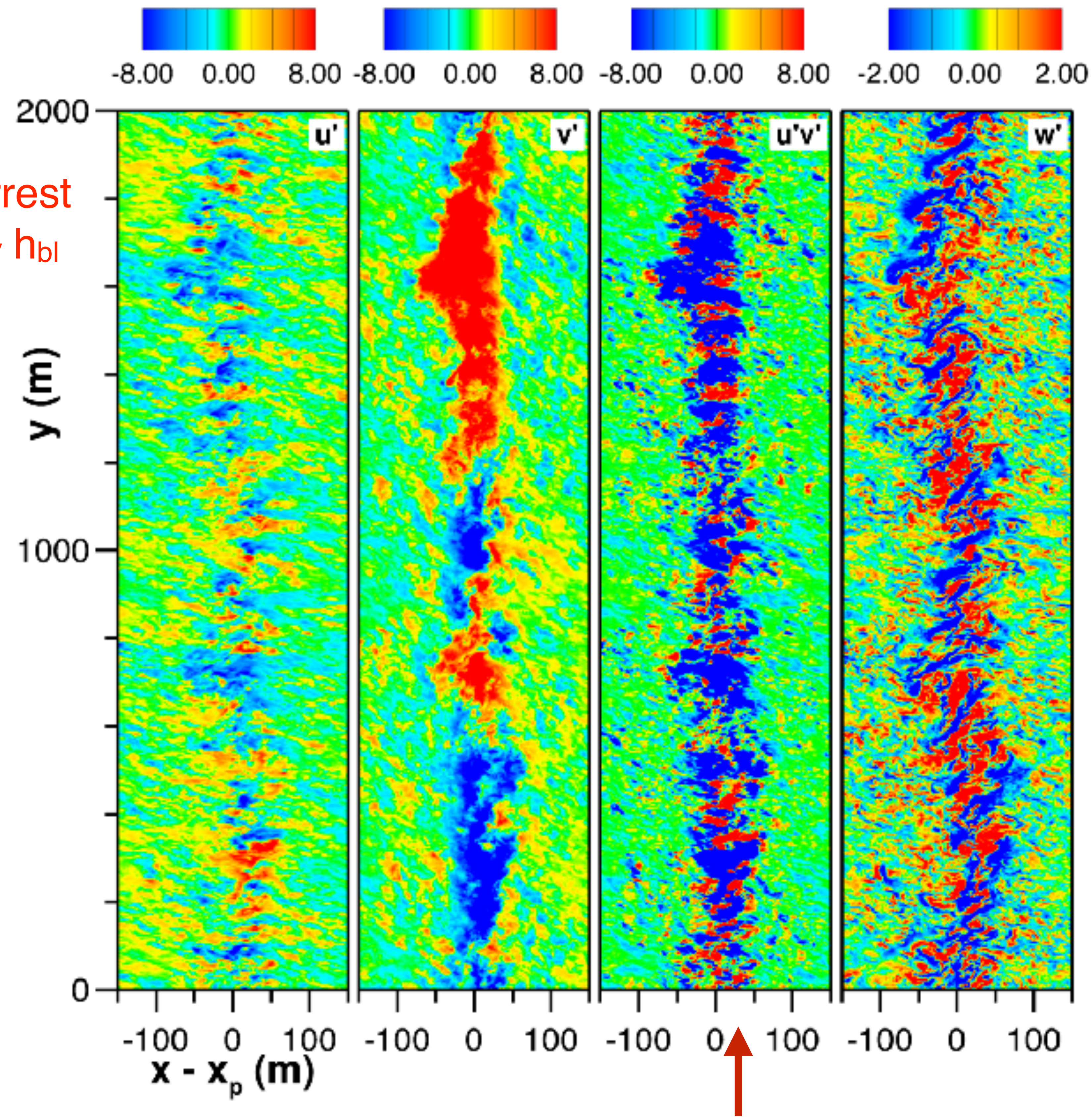

arrest by horizontal Reynolds stress, <u'v'> < 0

alongfront wavenumber spectrum at time of peak arrest

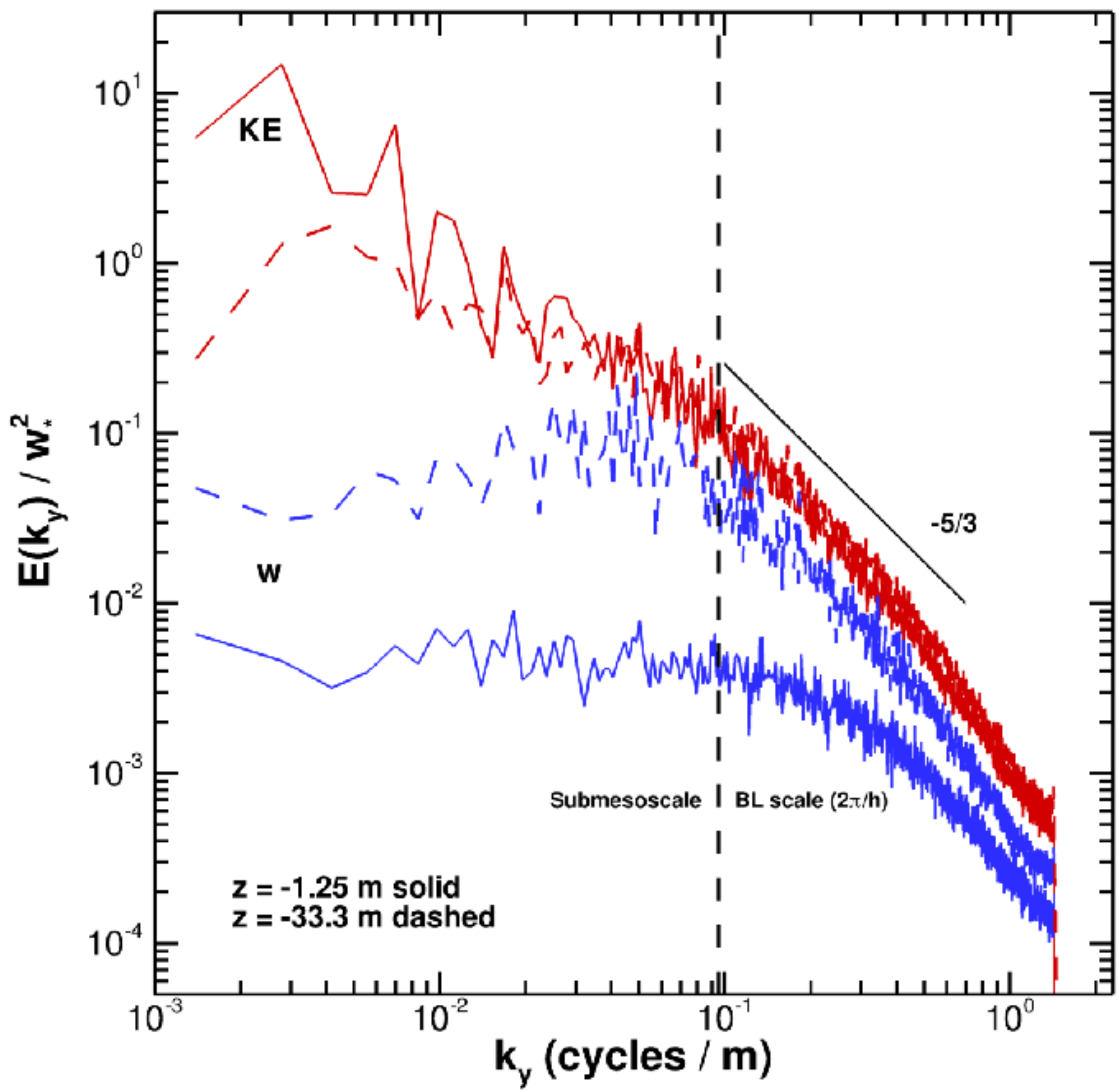

Different LES cases: E and N winds and free convection:

TTW frontogenesis, arrest, and decay always happen, but differently in detail

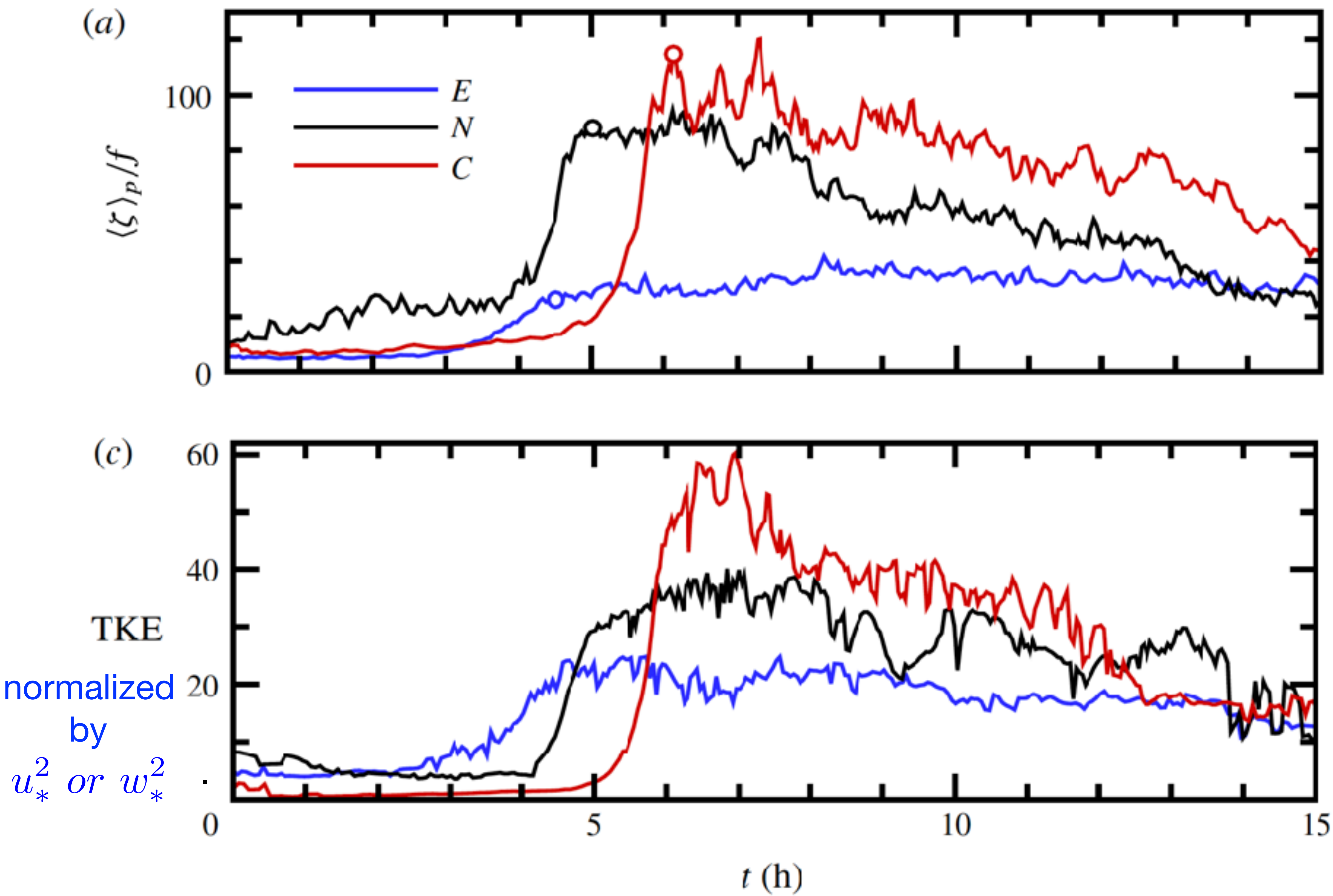

Surface Gravity Wave-Averaged Effects on Currents (WEC)

$$\begin{aligned} \partial_t \mathbf{u} \; + \ldots \;&=\; \mathbf{u}_{st} \times (f\hat{\mathbf{z}} + \nabla \times \mathbf{u}) + \mathbf{F}^w \\ \partial_t C \; + \ldots \;&=\; -\,\mathbf{u}_{st} \cdot \nabla C + Q^w \\ \nabla \cdot \mathbf{u} \;&=\; \nabla \cdot \mathbf{u}_{st} \;=\; 0\,. \end{aligned}$$

wave-added terms

$\mathbf{u}$ ... 3D wave-averaged velocity

$\mathbf{u}_{st}$ ... 3D Stokes drift

C ... wve-averaged material tracer (including bouyancy)

$\mathbf{F}^w$ ... non-conservative wave-related force (often Radiation Stress
. divergence, but also added mixing)

Q^w ... non-conservative wave-related effects on C, mostly mixing

Now proceed to do similar SCFT diagnoses, ROMS simulations, and LES with WEC.

Filament in Wind-Wave Equilibrium: **S**econdary **C**irculation

$$\theta_{wind} = \theta_{wave} = \frac{\pi}{4}$$

with WEC

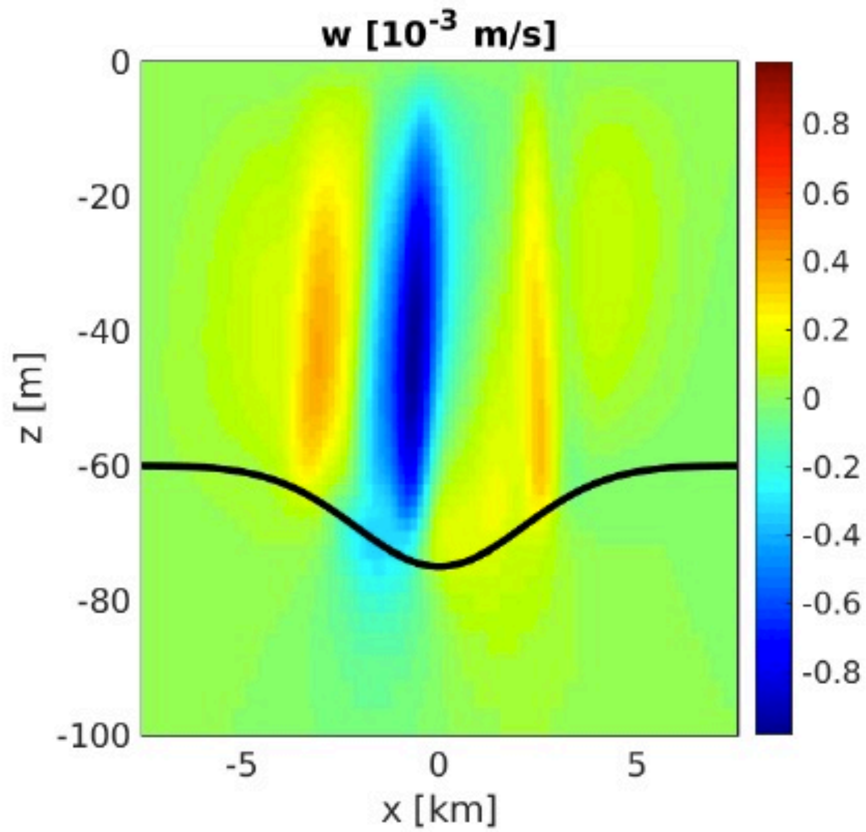

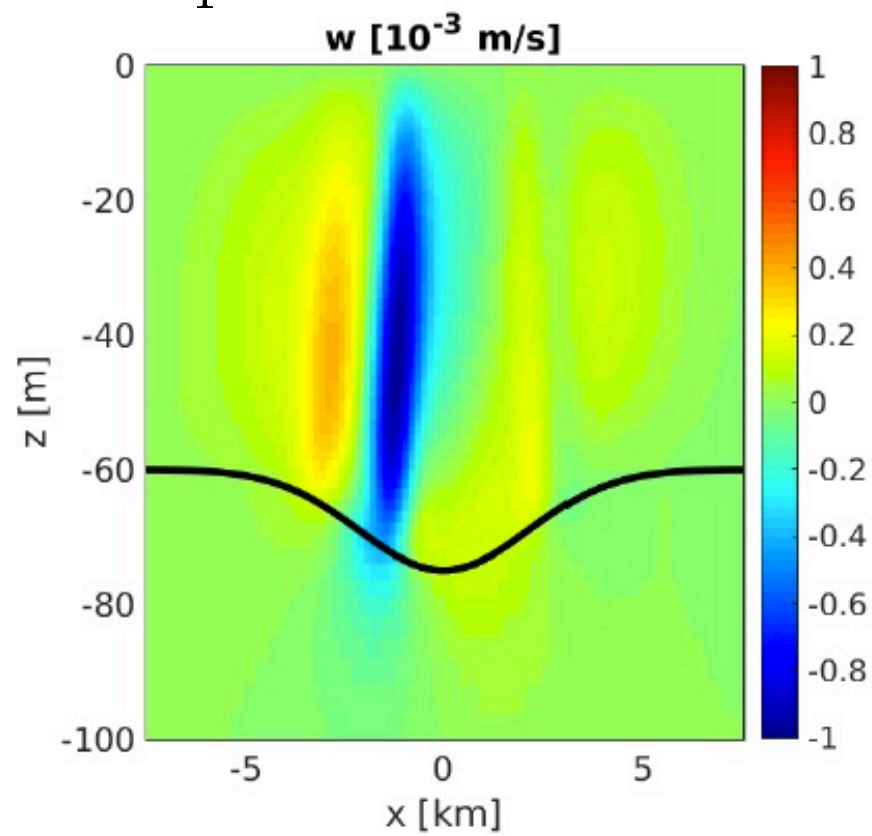

without WEC

difference field

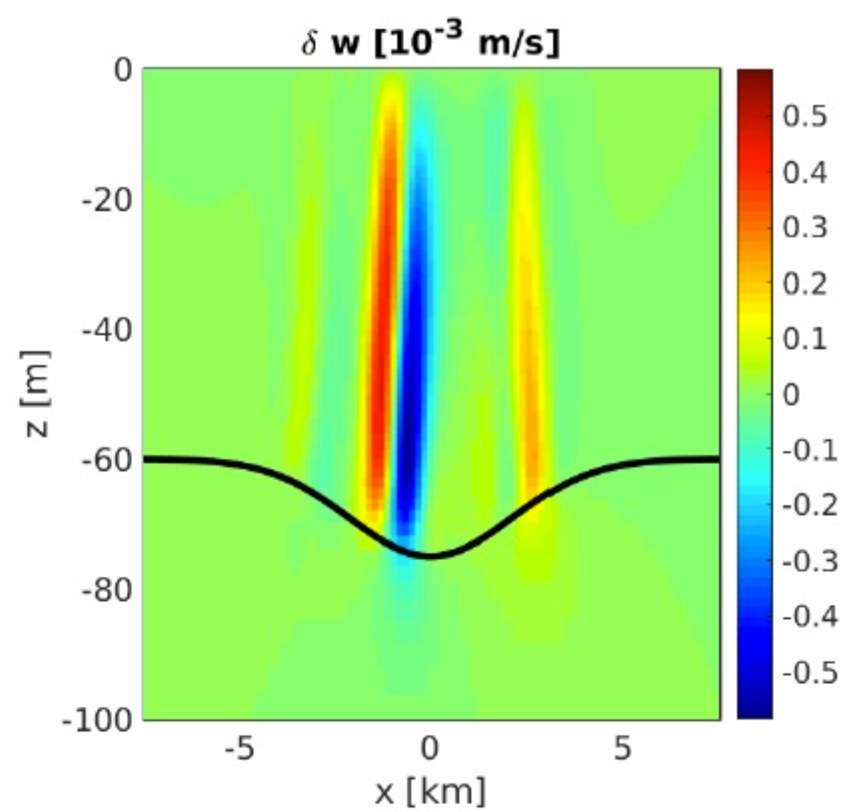

fully nonlinear SCFT with TTW and WEC and Ekman currents

w here is stronger than with either TTW or WEC alone through constructive alignment with Ekman current

(McWilliams, 2018)

Filament in Wind-Wave Equilibrium: **F**rontogenetic **T**endency

$$\theta_{wind} = \theta_{wave} = \frac{\pi}{4}$$

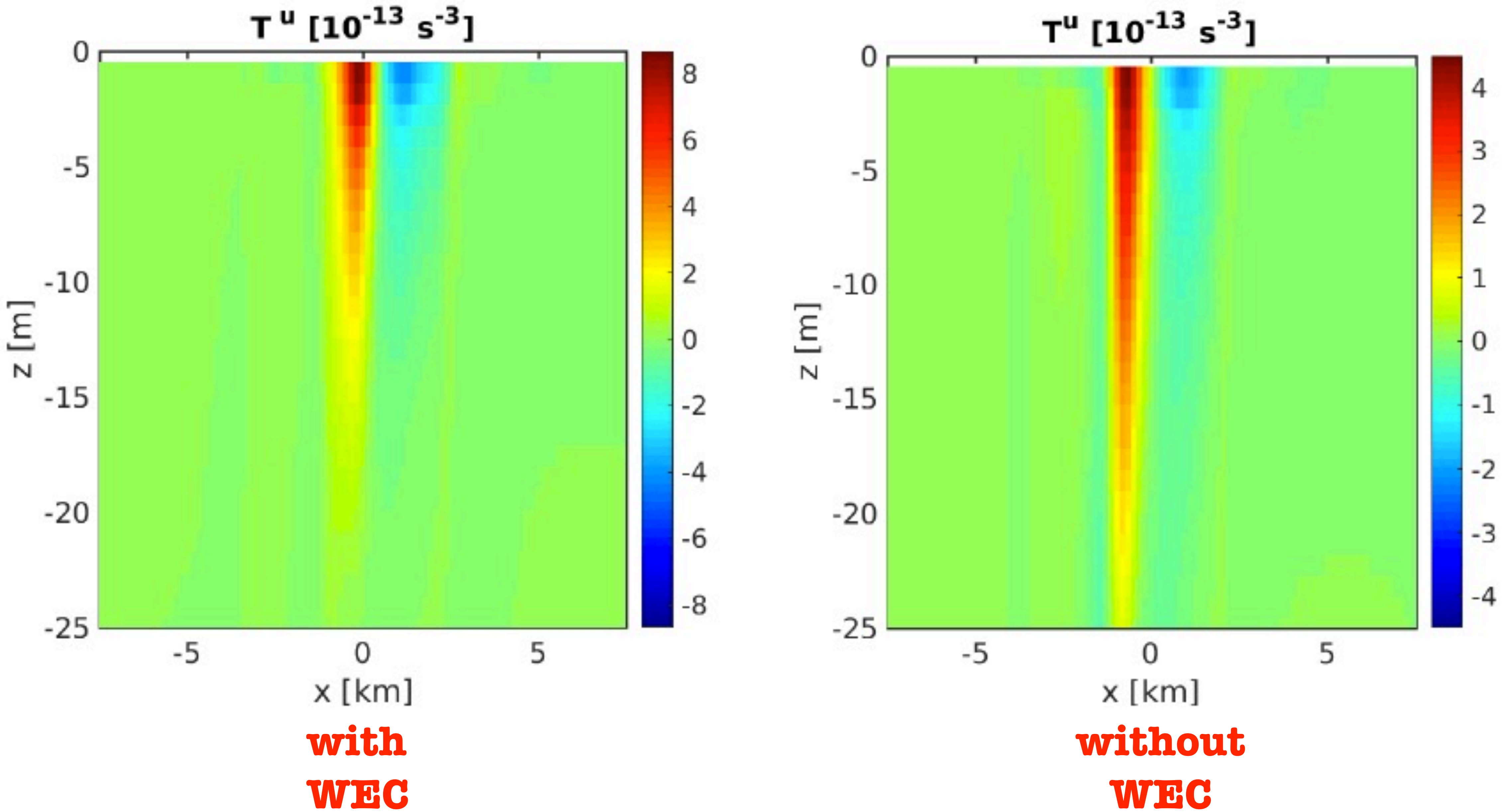

T^u here is stronger than with either TTW or WEC alone through constructive alignments with Ekman current and ageostrophic advection.

Filament Frontogenesis in LES with Surface Waves

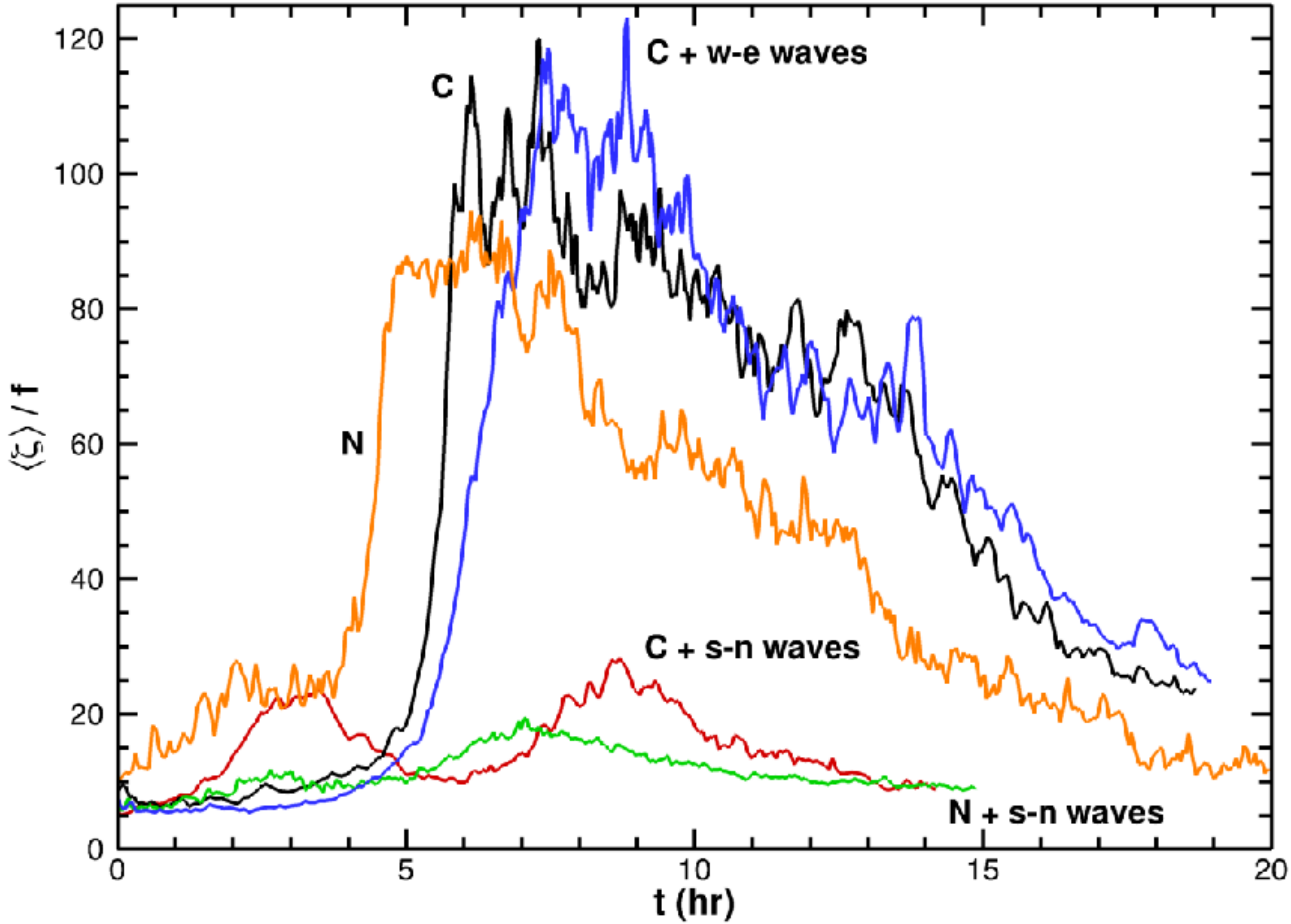

(Sullivan and McWilliams, 2018)

Why is TTW frontogenesis made so much weaker with along-front waves?

Because the wave forces induce a shallow eastward geostrophic flow in the filament center that tears of the top of the front by eastward advection:

$$\partial_t u \;=\; \cdots + \int_{-\infty}^{z} \partial_z v^{st}\;\zeta\;dz' \;>\; 0$$

with $v^{st},\ \zeta\ >\ 0$. This has the effect of creating two east-side fronts with competing secondary circulations, hence “detuning” the frontogenesis.

alongfront-averaged vertical velocity after frontal rragmentation

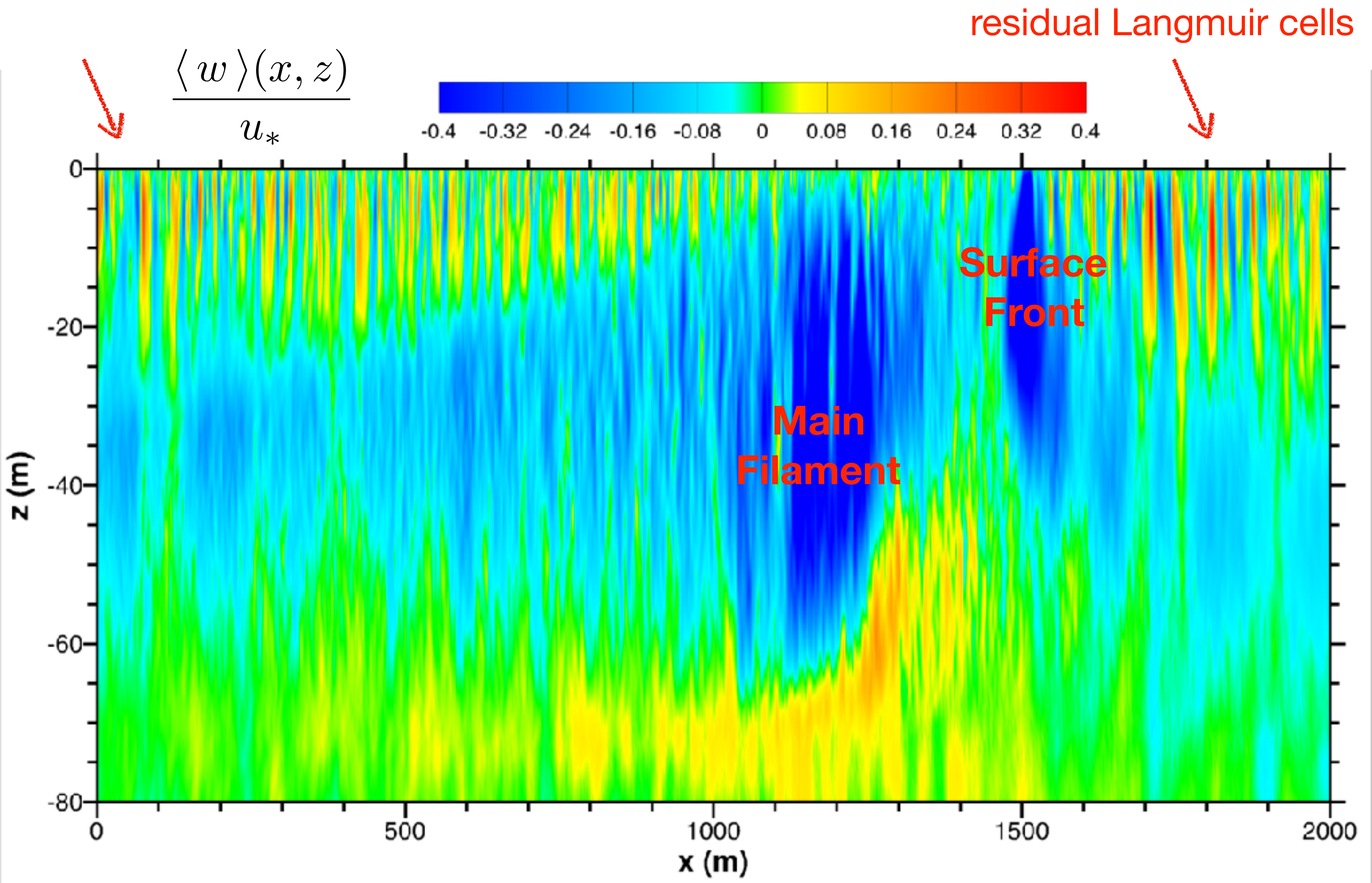

w(x,y) at z = - 5 m after frontal fragmentation: inhomogeneous Langmuir turbulence

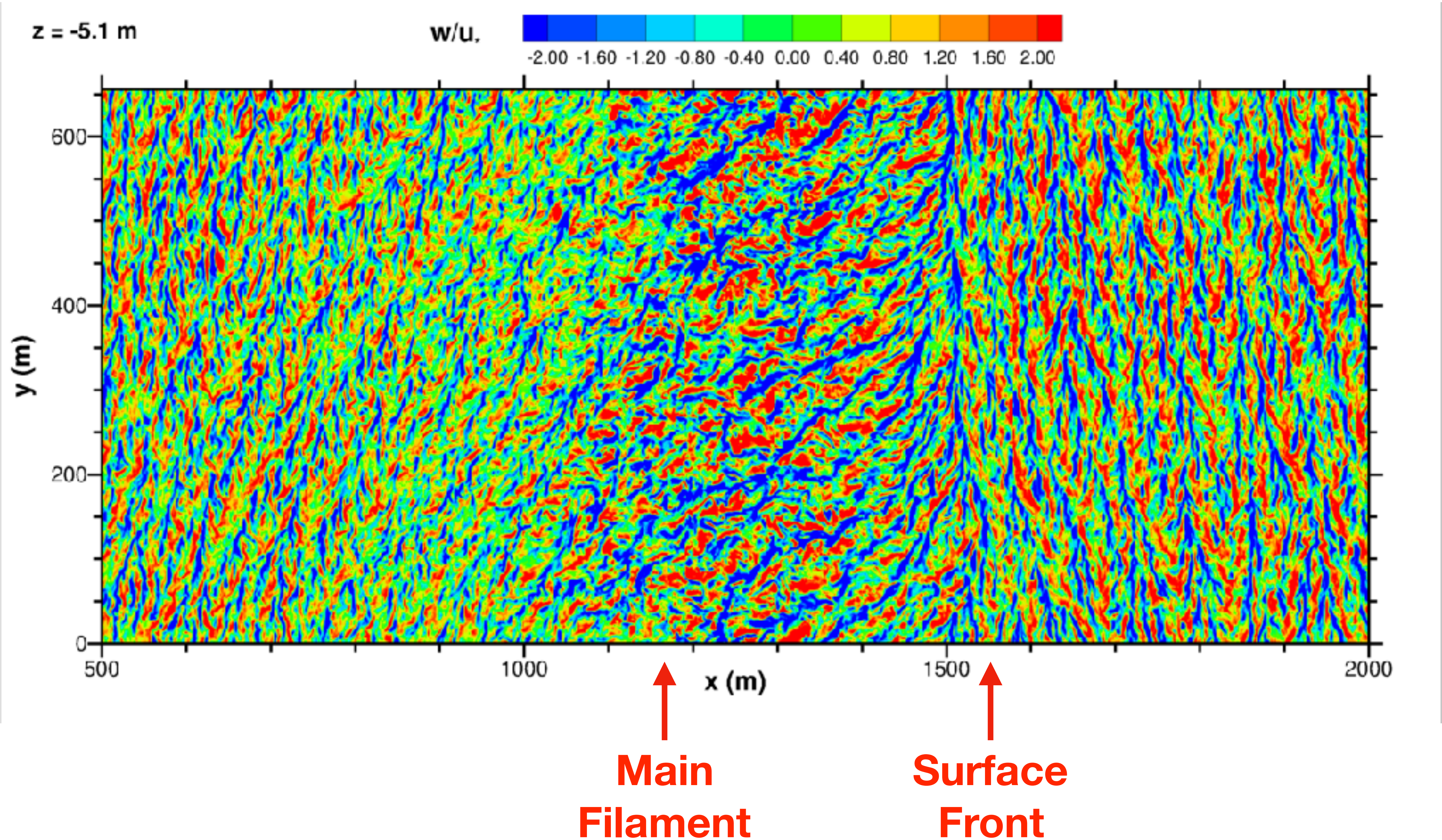

Summary

frontogenesis (FG) is a key process for surface submesoscale currents

in realistic simulations TTW-induced convergence is more common than mesoscale strain as a cause of FG

“balanced” diagnoses from b and ν_v (or background strain rate) —> Secondary Circulation and Frontogenetic Tendencies (SCFT)

surface convergence δ associated with the frontal ageostrophic secondary circulation is the cause of strong FG (Ro > 1) over a time of a few hrs.

frontal arrest is often caused by lateral shear instability

frontal arrest set the lower size limit for the submesoscale regime, here with a width ~ h_{BL}

frontal decay extends over several days with slowly weakening currents

surface waves' Stokes drift has an important influence on strong fronts

we don't yet have a phenomenological overview of submesoscale <-> surface wave <-> boundary-layer interactions, but vertical momentum mixing is key to FG